

# Extraction and Approximation of Range Image Data Using a Rational Bézier Surface \*

Iwao SEKITA (sekita@etl.go.jp)  
Information Science Div.  
Electrotechnical Laboratory (ETL)  
Tsukuba, Ibaraki, Japan 305

Pierre Boulanger and Guy Godin  
Inst. Information Technology  
National Research Council of Canada (NRC)  
Ottawa, Ontario, Canada K1A0R6

## Abstract

*This paper presents a new method for the extraction of a rational Bézier surface from a set of data points. The algorithm is divided in three parts. First, a least median square fitting algorithm is used to extract a Bézier surface from the data set. Secondly, from this initial surface model an analysis of the data set is performed to eliminate outliers. Thirdly, the algorithm then improves the fit over the residual points by modifying the weights of a rational Bézier surface using a non-linear optimization method. A further improvement of the fit is achieved using a new intrinsic parametrization technique. Experimental results show that the current algorithm is robust and can precisely approximate complex surfaces.*

## 1. Introduction

Creation of a geometric CAD model is usually one of the most complex parts of computer-based design and analysis systems. For objects with geometric regularity, it is practical to generate them interactively, using one of several geometric modelling schemes. However, there are many areas in which there is a need to create a database by extracting an object definition from a complex real life object, i.e., one that already exists and which does not have regular geometric properties. Examples of such objects are found in the field of medicine (prostheses, plastic surgery), in industrial applications (reverse engineering and casting measurements), as well as in computer simulation (automatic definition of a mesh for finite element analysis). In order to satisfy these requirements a new reverse engineering package is under development. One can find an overview of the technologies developed so far in [1]. It is composed of an interactive acquisition module, a semi-automatic segmenter, an interface to CAD/CAM systems through a standard graphic description language (IGES), and an automatic replication module. This paper presents new results in one of the key technologies necessary to develop such a system.

Automatic segmentation methods based on histogram mode seeking (e.g., [2], [3]), region growing (e.g., [4], [5], [3], [6] [7]), and edge detection (e.g., [8], [9]), etc. have been proposed. One of the drawbacks

of such algorithms is the difficulty of entering in the segmentation process, high level requirements which are usually defined by the field of application. This is the reason why most commercial reverse engineering packages are fully manual.

In this paper, a semi-automatic segmentation method which adapts the request of users to the segmentation process is proposed. Such extraction methods were previously demonstrated by Roth [10] for implicit surfaces. One of the key requirements is the ability to roughly mark a region of interest and to extract the dominant surface from this data set. This requirement is essential since precise marking of a region has been known to be very difficult.

This paper presents a new method which satisfies the above requirement if certain assumptions are made. The main assumption is that the original data set can be approximately represented by a Bézier surface extracted by a least median square algorithm [11]. This assumption is reasonable since a Bézier surface is a rational Bézier with all the weights equal to one and that the precision of the fit can always be improved by varying these weights. The algorithm is divided in three main parts. First, a robust fit of a Bézier surface is extracted using a least median square algorithm. Second, a subset of the original data set is produced using an outlier detection algorithm. Third, from this data set, the weights of the rational Bézier are modified using a non-linear optimization algorithm. A further improvement of the precision is also obtained by using a new intrinsic parametrization algorithm.

In Section 2, we will review the basic definition of a rational Bézier surface. Section 3 will describe in detail the fitting algorithm. In Section 4, some experimental results are presented and Section 5 gives a summary and conclusion.

## 2. Rational Bézier Surface

Let us define a two-dimensional  $(u, v)$ -parameter plane. A rational Bézier surface  $\bar{s}(u, v)$  of degrees

\*NRC-35090

$(m_1 \times m_2)$  is defined by

$$\bar{s}(u, v) := \frac{\sum_{i=0}^{m_1} \sum_{j=0}^{m_2} w_{ij} \bar{p}_{ij} B_{i,m_1}(u) B_{j,m_2}(v)}{\sum_{i=0}^{m_1} \sum_{j=0}^{m_2} w_{ij} B_{i,m_1}(u) B_{j,m_2}(v)}, \quad (1)$$

$$B_{i,m}(t) := \frac{m!}{(m-i)!i!} t^i (1-t)^{(m-i)}$$

where  $w_{ij} \in R^1$  and  $\bar{p}_{ij} \in R^3$  are called a weight and a control point, respectively.

Let the numerator and the denominator of the rational Bézier surface  $\bar{s}(u, v)$  be  $\bar{A}(u, v)$  and  $D(u, v)$ , respectively, and define

$$\bar{q}_{ij} := w_{ij} \bar{p}_{ij}.$$

Then Eq. (1) can be written as:

$$\bar{s}(u, v) = \frac{\sum_{i=0}^{m_1} \sum_{j=0}^{m_2} \bar{q}_{ij} B_{i,m_1}(u) B_{j,m_2}(v)}{\sum_{i=0}^{m_1} \sum_{j=0}^{m_2} w_{ij} B_{i,m_1}(u) B_{j,m_2}(v)} = \frac{\bar{A}(u, v)}{D(u, v)}. \quad (2)$$

Partial derivatives are given by

$$\frac{\partial \bar{s}(u, v)}{\partial u} = \left( \frac{\partial \bar{A}(u, v)}{\partial u} - \frac{\partial D(u, v)}{\partial u} \bar{s}(u, v) \right) / D(u, v), \quad (3)$$

$$\frac{\partial \bar{s}(u, v)}{\partial v} = \left( \frac{\partial \bar{A}(u, v)}{\partial v} - \frac{\partial D(u, v)}{\partial v} \bar{s}(u, v) \right) / D(u, v), \quad (4)$$

where

$$\frac{\partial \bar{A}(u, v)}{\partial u} = m_1 \sum_{i=1}^{m_1} \sum_{j=0}^{m_2} (\bar{q}_{ij} - \bar{q}_{i-1,j}) B_{i,m_1-1}(u) B_{j,m_2}(v),$$

$$\frac{\partial D(u, v)}{\partial u} = m_1 \sum_{i=1}^{m_1} \sum_{j=0}^{m_2} (w_{ij} - w_{i-1,j}) B_{i,m_1-1}(u) B_{j,m_2}(v),$$

$$\frac{\partial \bar{A}(u, v)}{\partial v} = m_2 \sum_{i=0}^{m_1} \sum_{j=1}^{m_2} (\bar{q}_{ij} - \bar{q}_{i,j-1}) B_{i,m_1}(u) B_{j,m_2-1}(v),$$

$$\frac{\partial D(u, v)}{\partial v} = m_2 \sum_{i=0}^{m_1} \sum_{j=1}^{m_2} (w_{ij} - w_{i,j-1}) B_{i,m_1}(u) B_{j,m_2-1}(v).$$

Rational Bézier surfaces are commonly used in CAD systems and are general surfaces capable of representing a large range of surface primitives. It is also known that conic sections [12] can be exactly expressed by rational Bézier functions.

### 3. Surface Extraction and Approximation

In this algorithm, we first extract a Bézier surface from the data set selected by the user, by setting all the weights equal to one. The extraction routine is based on a least median square algorithm first proposed by Rousseeuw [11]. This algorithm is robust up to 50% outliers and can be computed quite efficiently. Following this extracted Bézier surface, we then eliminate from the original data set the points considered to be outliers. From the residual data set, we then optimize the weight values using a non-linear optimization technique. We also improve the accuracy of the fit by using an intrinsic parametrization algorithm.

#### 3.1. Robust Fitting of a Bézier Surface

Let  $\{x_k\}_{k \in C_x}$  and  $\{y_k\}_{k \in C_y}$  be a set of measurements of a smooth surface and its background, respectively. One can observe only  $\{\tilde{z}_k\}_{k \in C_0}$ , where  $\{\tilde{z}_k\}_{k \in C_0} = \{\tilde{x}_k\}_{k \in C_x} \cup \{\tilde{y}_k\}_{k \in C_y}$ ,  $\tilde{x}_k = x_k + \varepsilon_k$ ,  $C_x \cup C_y = C_0$ ,  $C_x \cap C_y = \emptyset$ , and  $\varepsilon_k$  is a random noise subject to a normal distribution with mean 0 and standard deviation  $\sigma$ . Suppose that  $\{f_k\}_{k \in C_0}$  is obtained by least median fitting and  $f_k = x_k$  ( $k \in C_x$ ). Then consider the ratio  $|C_x|/(|C_x| + |C_y|)$  when  $|f_k - \tilde{y}_k| \geq 2\sigma$  ( $k \in C_y$ ) and the median of  $\{|f_k - \tilde{z}_k\}_{k \in C_0}$  is asymptotically less than or equal to  $2\sigma$ . The value of this ratio for these conditions is equal to:

$$|C_x|/(|C_x| + |C_y|) \geq 0.524.$$

Here the notation  $|C_x|$  means the number of elements of class  $C_x$ . When  $|f_k - \tilde{y}_k| \geq \sigma$  ( $k \in C_y$ ) and the median of  $\{|f_k - \tilde{z}_k\}_{k \in C_0}$  is asymptotically less than or equal to  $\sigma$  the same ratio is equal to:

$$|C_x|/(|C_x| + |C_y|) \geq 0.733.$$

Here approximate values of the probability are equal to:

$$2 \int_{2\sigma}^{\infty} (1/\sqrt{2\pi\sigma^2}) \exp\{-x^2/(2\sigma^2)\} dx \approx 0.04550 \text{ and } 2 \int_{\sigma}^{\infty} (1/\sqrt{2\pi\sigma^2}) \exp\{-x^2/(2\sigma^2)\} dx \approx 0.3173.$$

The method of robust fitting of a Bézier surface of degrees  $(m_1 \times m_2)$  based on the least median consists of the following four steps:

- 1 Measure uniformly-parametrized 3-D data ( $\Omega_0 := \{\tilde{z}_{kl}\}_{kl \in C_0} = \{[\tilde{z}_{0,kl}, \tilde{z}_{1,kl}, \tilde{z}_{2,kl}]^T\}_{kl \in C_0}$ ), where  $Z^T$  denotes the transpose of  $Z$ ).
- 2 For  $t = 0$  to  $n_1$

- 2.1 Randomly extract  $(m_1 + 1)$  points  $\{u_{k(t)}\}_{k=0}^{m_1}$  in  $u$ -axis and  $(m_2 + 1)$  points  $\{v_{l(t)}\}_{l=0}^{m_2}$  in  $v$ -axis. Let  $\Omega_1$  be  $\{\tilde{z}_{k(t)l(t)}\}_{k=0}^{m_1} \{l=0\}^{m_2}$ .
- 2.2 Calculate a Bézier surface

$$\bar{f}(u, v) = \sum_{i=0}^{m_1} \sum_{j=0}^{m_2} \bar{p}_{ij} B_{i,m_1}(u) B_{j,m_2}(v) \text{ by the}$$

tensor product approach, which interpolates  $\Omega_1$ . That is, the coefficients  $P$ ,

$$\bar{p}_{ij} =: [p_{0,ij}, p_{1,ij}, p_{2,ij}]^T, \quad P := [P_0, P_1, P_2],$$

$$P_\lambda := \begin{bmatrix} p_{\lambda,00}, & p_{\lambda,01}, & \dots, & p_{\lambda,0m_2} \\ p_{\lambda,10}, & p_{\lambda,11}, & \dots, & p_{\lambda,1m_2} \\ \dots & \dots & \dots & \dots \\ p_{\lambda,m_1 0}, & p_{\lambda,m_1 1}, & \dots, & p_{\lambda,m_1 m_2} \end{bmatrix},$$

of the surface is obtained by the following:

1) Obtain  $Q$  by solving linear equations:

$$U[Q_0, Q_1, Q_2] = [Z_0, Z_1, Z_2], \quad (5)$$

where

$$Z_\lambda := \begin{bmatrix} \tilde{z}_{\lambda,0(t)0(t)}, & \dots, & \tilde{z}_{\lambda,0(t)m_2(t)} \\ \tilde{z}_{\lambda,1(t)0(t)}, & \dots, & \tilde{z}_{\lambda,1(t)m_2(t)} \\ \dots & \dots & \dots \\ \tilde{z}_{\lambda,m_1(t)0(t)}, & \dots, & \tilde{z}_{\lambda,m_1(t)m_2(t)} \end{bmatrix},$$

$$U := \begin{bmatrix} B_{0,m_1}(u_0(t)), & \dots, & B_{m_1,m_1}(u_0(t)) \\ B_{0,m_1}(u_1(t)), & \dots, & B_{m_1,m_1}(u_1(t)) \\ \dots & \dots & \dots \\ B_{0,m_1}(u_{m_1}(t)), & \dots, & B_{m_1,m_1}(u_{m_1}(t)) \end{bmatrix}.$$

2) And obtain  $P$  by solving linear equations:

$$V^T [P_0^T, P_1^T, P_2^T] = [Q_0^T, Q_1^T, Q_2^T], \quad (6)$$

where

$$V := \begin{bmatrix} B_{0,m_2}(v_0(t)), & \dots, & B_{0,m_2}(v_{m_2}(t)) \\ B_{1,m_2}(v_0(t)), & \dots, & B_{1,m_2}(v_{m_2}(t)) \\ \dots & \dots & \dots \\ B_{m_2,m_2}(v_0(t)), & \dots, & B_{m_2,m_2}(v_{m_2}(t)) \end{bmatrix}.$$

2.3 Calculate the median of residuals for the subset  $\Omega_2$  of  $\Omega_0$  without  $\Omega_1$  (in order to calculate more quickly). Here, a selection method based on the quick-sort algorithm can be used [13].

2.4 If the median is smaller than the previous least median,

**then** store the median as the least median until now and store  $P$ .

3 Determine the Bézier surface with the least median.

4 Regard not only the region ( $\Omega_3$ ) with

$$\|\tilde{f}(u_k, v_l) - \tilde{z}_{kl}\|^2 > T_1 \quad (7)$$

but also sub-regions as an outliers (background), because most of sub-regions may be intersections of the Bézier surface and the background surface. The sub-regions can be removed by using the opening operation of digital morphology [14]. Let suppose that the main surface region has at least  $(2m_3 + 1)$  pixels in  $u$ -direction and at least  $(2m_4 + 1)$  pixels in  $v$ -direction on the  $(u, v)$ -plane. The set  $\Omega_4$  is obtained as a set of subscript of 1-valued pixels of  $\text{OPEN}(I_Z, I_{H_1})$ :

$$\text{OPEN}(I_Z, I_{H_1}) = \bigvee \{ \text{TRAN}(I_{H_1}; k, l) :$$

$$\text{TRAN}(I_{H_1}; k, l) \subseteq I_Z \}, \quad (8)$$

$$I_Z(k, l) := \begin{cases} 1 & \|\tilde{f}(u_k, v_l) - \tilde{z}_{kl}\|^2 \leq T_1 \\ 0 & \text{otherwise,} \end{cases}$$

$$I_{H_1}(k, l) := \begin{cases} 1 & |k| \leq m_3 \text{ and } |l| \leq m_4 \\ 0 & \text{otherwise,} \end{cases}$$

$$\text{TRAN}(I(k, l); i, j) := I(k - i, l - j).$$

And  $I_1 \subseteq I_2$  denotes that  $I_1$  is a subimage of  $I_2$ . Let the result of the opening operation be denoted by  $o_{kl}$  ( $= \tilde{z}_{kl}$ ) ( $kl \in \Omega_4$ ) and be called a initial surface region.

The trial number  $n_1$  depends on the ratio  $|C_x|/(|C_x| + |C_y|)$ . The probability that all  $(m_1 + 1)(m_2 + 1)$  points are extracted from  $C_x$  with  $\varepsilon_{kl} < \sigma$  is about  $(\frac{0.682|C_x|}{|C_x| + |C_y|})^{(m_1+1)(m_2+1)}$ . Therefore  $n_1 > (\frac{1}{\tilde{r}_m})^{(m_1+1)(m_2+1)}$  is recommended, where  $\tilde{r}_m$  is the minimum estimate of  $|C_x|/(|C_x| + |C_y|)$ .

To determine the threshold  $T_1$  automatically, let us consider the least median  $\nu_x$ . If  $|C_x|/(|C_x| + |C_y|) = 1$ , the least median  $\nu_x$  is expected to be the median  $\nu$  of the absolute value of the random variable, subject to the normal distribution with mean 0 and standard deviation  $\sigma$ . It is numerically obtained as the point such that the integral value of the normal density function from 0 to  $\nu$  equals the integral value from  $\nu$  to the infinity, which is about  $0.67449\sigma$ . If  $|f_{kl} - \tilde{y}_{kl}| \geq 0.67449\sigma$  ( $k \in C_y$ ), the least median is equal to  $\nu_x \geq 0.67449\sigma$ . If  $T_1$  is set to  $2.5\sigma$  under the safety consideration that  $\nu_x = 0.67449\sigma$ ,

$$T_1 = 2.5\sigma = (2.5/0.67449)\nu_x \quad (9)$$

is obtained.

### 3.2. Approximation by a Rational Bézier Surface

In this subsection, a method for approximating the extracted surface model in subsection 3.1 by a rational Bézier surface is shown with proposed intrinsic parametrization.

A Bézier surface is the special case when all weights  $w_{ij}$  of a rational Bézier surface are equal to 1. Here, weights  $w_{ij}$  and coefficients  $\tilde{q}_{ij}$  are determined by iterative and alternate calculations. The weights  $w_{ij}$  are modified by the Newton method on the condition that  $\tilde{q}_{ij}$  are fixed. Using the notations

$$\vec{w} := [w_{00}, w_{01}, \dots, w_{0m_2}, w_{10}, w_{11}, \dots, w_{m_1 m_2}]^T, \quad \vec{s}_{kl} := \vec{s}(u_k, v_l), \quad \sum_{ij} := \sum_{i=0}^{m_1} \sum_{j=0}^{m_2}, \quad R := E_{kl \in \Omega_4} \|\vec{s}_{kl} - \vec{o}_{kl}\|^2$$

and an arithmetic expectation operator  $E_{kl \in \Omega_4} := \frac{1}{|\Omega_4|} \sum_{kl \in \Omega_4}$ , the weights  $\vec{w}$  update equation is then equal

to:

$$\vec{w} \leftarrow \vec{w} - F^{-1} \nabla \vec{f}, \quad (10)$$

$$F := \frac{1}{2} \begin{bmatrix} \frac{\partial^2 R}{\partial w_{00} \partial w_{00}}, & \dots, & \frac{\partial^2 R}{\partial w_{m_1 m_2} \partial w_{00}} \\ \vdots & & \vdots \\ \frac{\partial^2 R}{\partial w_{00} \partial w_{m_1 m_2}}, & \dots, & \frac{\partial^2 R}{\partial w_{m_1 m_2} \partial w_{m_1 m_2}} \end{bmatrix},$$

$$\nabla \vec{f} := \frac{1}{2} \left[ \frac{\partial R}{\partial w_{00}}, \dots, \frac{\partial R}{\partial w_{m_1, m_2}} \right]^T,$$

$$\frac{1}{2} \frac{\partial R}{\partial w_{i_0 j_0}} = \mathbb{E}_{k_l \in \Omega_4} (\vec{s}_{kl} - \vec{o}_{kl})^T \frac{\partial \vec{s}_{kl}}{\partial w_{i_0 j_0}},$$

$$\frac{\partial \vec{s}_{kl}}{\partial w_{i_0 j_0}} = -\vec{s}_{kl} b_{i_0 j_0 k l},$$

$$b_{i_0 j_0 k l} := \frac{B_{i_0, m_1}(u_k) B_{j_0, m_2}(v_l)}{\sum_{ij} w_{ij} B_{i, m_1}(u_k) B_{j, m_2}(v_l)},$$

$$\frac{1}{2} \frac{\partial^2 R}{\partial w_{i_1 j_1} \partial w_{i_0 j_0}} = \mathbb{E}_{k_l \in \Omega_4} \left\{ \frac{\partial \vec{s}_{kl}^T}{\partial w_{i_1 j_1}} \frac{\partial \vec{s}_{kl}}{\partial w_{i_0 j_0}} - 2 \left( \frac{1}{2} \frac{\partial R}{\partial w_{i_0 j_0}} \right) b_{i_1 j_1, k l} \right\}.$$

The control points  $\vec{q}_{ij}$  are calculated by a least mean squares method under the condition that  $w_{ij}$  are fixed. They are obtained by solving the linear equation:

$$\mathbb{E}_{k_l \in \Omega_4} \vec{b}_{kl} \vec{b}_{kl}^T Q = \mathbb{E}_{k_l \in \Omega_4} \vec{b}_{kl} \vec{o}_{kl}^T, \quad (11)$$

where

$$Q := [\vec{q}_{00}, \vec{q}_{01}, \dots, \vec{q}_{m_1, m_2}]^T,$$

$$\vec{b}_{kl} := \left[ \frac{B_{0, m_1}(u_k) B_{0, m_2}(v_l)}{\sum_{ij} w_{ij} B_{i, m_1}(u_k) B_{j, m_2}(v_l)}, \dots, \frac{B_{m_1, m_1}(u_k) B_{m_2, m_2}(v_l)}{\sum_{ij} w_{ij} B_{i, m_1}(u_k) B_{j, m_2}(v_l)} \right]^T.$$

Uniform parametrization is robust to noise; however, the residual between the approximation function  $\vec{s}_{kl}$  and the measurements  $\vec{o}_{kl}$  is not perpendicular to the tangent plane at each point  $\vec{s}_{kl}$ . Intrinsic parametrization means that each residual vector  $\vec{\delta}_{kl} := \vec{o}_{kl} - \vec{s}_{kl}$  becomes perpendicular to the tangent plane of the surface. It was introduced by Hoschek [15]. He implemented the parametrization by iteratively modifying the parameter as

$$u_k \leftarrow u_k + \Delta c_k / \alpha, \quad v_l \leftarrow v_l + \Delta d_l / \beta,$$

$$\Delta c_k = \vec{\delta}_{kl}^T \frac{\partial \vec{s}_{kl}}{\partial u} / \left| \frac{\partial \vec{s}_{kl}}{\partial u} \right|, \quad \Delta d_l = \vec{\delta}_{kl}^T \frac{\partial \vec{s}_{kl}}{\partial v} / \left| \frac{\partial \vec{s}_{kl}}{\partial v} \right|,$$

where  $\alpha$  is the approximative length of the parameter line  $u_k = \text{const.}$  and  $\beta$  is the approximative length of the parameter line  $v_l = \text{const.}$  However,  $\frac{\partial \vec{s}_{kl}}{\partial u}$  is not perpendicular to  $\frac{\partial \vec{s}_{kl}}{\partial v}$  and the ratio of the length of

the parameter to the length of a curve on the approximation function is dependent on the position. In this paper, the following modification is proposed:

$$u_k \leftarrow u_k + \Delta u_k, \quad v_l \leftarrow v_l + \Delta v_l. \quad (12)$$

Let  $\vec{\Delta}_{kl} := [\Delta u_k, \Delta v_l]^T$ ,  $\vec{\Delta}_{kl}$  be determined by

$$\min_{\vec{\Delta}_{kl}} \|[J_{kl}]^T \vec{\Delta}_{kl} - \vec{\delta}_{kl}\|^2,$$

where  $[J_{kl}]^T$  is a Jacobian matrix

$$[J_{kl}]^T = \left[ \frac{\partial \vec{s}_{kl}}{\partial u_k}, \frac{\partial \vec{s}_{kl}}{\partial v_l} \right]$$

which can be obtained by using Eqs. (3) and (4).

Then  $\vec{\Delta}_{kl}$  is obtained by

$$\vec{\Delta}_{kl} = ([J_{kl}][J_{kl}]^T)^{-1} [J_{kl}] \vec{\delta}_{kl}. \quad (13)$$

Here  $[J_{kl}][J_{kl}]^T$  is a  $(2 \times 2)$  matrix and its inverse matrix can be analytically computed. The modification value  $\vec{\Delta}_{kl}$  is the optimal estimate as far as one uses the first derivative, however there is a possibility that  $\|\vec{\delta}_{kl}(u_k + \Delta u_k, v_l + \Delta v_l)\|^2 > \|\vec{\delta}_{kl}(u_k, v_l)\|^2$ . In this case,  $\vec{\Delta}_{kl} \leftarrow \vec{\Delta}_{kl}/2$  is performed.

Let us consider one cycle of iteration of the above method:

Compute the intrinsic parametrization.

Optimize the weights using the Newton method.

Compute the intrinsic parametrization.

Refit using least mean squares method.

Compute the intrinsic parametrization.

Refit using the least mean squares method.

As a convergence criterion for the above cycle, one can use a least mean squares error criteria

$$R = \mathbb{E}_{k_l \in \Omega_4} \vec{o}_{kl}^T \vec{o}_{kl} - \text{trace}(Q^T \mathbb{E}_{k_l \in \Omega_4} \vec{b}_{kl} \vec{o}_{kl}^T), \quad (14)$$

and the mean absolute angles between the residual and two axes of the tangent plane

$$\mathbb{E}_{k_l \in \Omega_4} \left| \arccos \left( \frac{\frac{\partial \vec{s}_{kl}^T}{\partial u_k} \vec{\delta}_{kl}}{\left| \frac{\partial \vec{s}_{kl}^T}{\partial u_k} \right| \|\vec{\delta}_{kl}\|} \right) \right|, \quad \mathbb{E}_{k_l \in \Omega_4} \left| \arccos \left( \frac{\frac{\partial \vec{s}_{kl}^T}{\partial v_l} \vec{\delta}_{kl}}{\left| \frac{\partial \vec{s}_{kl}^T}{\partial v_l} \right| \|\vec{\delta}_{kl}\|} \right) \right|,$$

where the numerator of the argument of "arccos" is obtained in  $[J_{kl}] \vec{\delta}_{kl}$  in Eq.(13). In Section 4, the relative least mean squares error

$$\frac{R_{new}}{R_{old}} \geq T_2 \quad (15)$$

was used.

### 3.3. Extraction of a Single Connected Surface

In this subsection, a method of determining a final region of the data set corresponding to the largest connected component is presented.

The dominant region is expected to be smaller or equal than the initial region indicated by  $\Omega_4$ . Therefore, a candidate region of the object is obtained by dilation of the region ( $\Omega_4$ ). It can be performed by the binary dilation [14] of the region  $\Omega_4$ , e.g.,  $m_5$ -pixel-dilated region indicated by  $\Omega_5$  is obtained as 1-valued pixels of  $DILATE(I_Z, I_{H_2})$ :

$$DILATE(I_Z, I_{H_2}) = \bigvee_{(k,l) \in \Omega_4} TRAN(I_{H_2}; k, l), \quad (16)$$

$$I_{H_2}(k, l) := \begin{cases} 1 & k^2 + l^2 \leq m_5^2 \\ 0 & \text{otherwise.} \end{cases}$$

The region  $\Omega_5$  is obtained after the robust fitting of a Bézier surface in subsection 3.1, and the intrinsic parametrization in subsection 3.2 is applied. The Newton method and the least mean squares method are applied to the region indicated by  $\Omega_4$  in subsection 3.2.

For the region indicated by  $\Omega_5$ , we consider not only points with  $\|\vec{s}(u_k, v_l) - \vec{z}_{kl}\|^2 > T_3$  but also sub-regions as an outlier (background). Here the threshold  $T_3$  is set to, e.g.,  $3\sqrt{R}$ .

### 4. Experiments

The NRC range image data files [16] were used to illustrate the property of the algorithm. The first image used is cat #105 and contains simple geometrical objects (see Figure 1). One can see in Figure 2 the rough marking performed by the operator. Figure 3 shows the complement of regions named region  $\Omega_3$  in step 4 in subsection 3.1. Here, the threshold  $T_1$  was automatically given by Equation (9). Degrees of the Bézier surface were  $m_1 = 2$  and  $m_2 = 2$ . The selection of degrees is important, because it is directly related to the ability to approximate. If  $m_1 = m_2 = 1$  then the curved surfaces such as a sphere or a cylinder can not be represented. If  $m_1$  and  $m_2$  are very large, the Bézier surface can approximate the background as well as the dominant surface, and the background does not become the outlier. Figure 4 shows the dominant regions after removing sub-regions from the surface illustrated in Figure 3 using the opening operation, where  $m_3 = m_4 = 1$ . Figure 5 shows the approximation results of the data set using the *rational* Bézier surface fitting algorithm discussed in subsection 3.2, where  $T_2 = 0.995$  of Eq. (15) and  $m_5 = 3.5$  of Eq. (16). Figure 6 shows the final connected component region where the boundary are highlighted. It is shown from the above examples that a simple object like a cylinder or a sphere are well extracted by the proposed method even though a non-rational Bézier surface was used in the least median fitting.

Figure 7 shows an example of more complex object (telephone) from cat #028. Figure 8(a) is a user specified region, and Fig. 8(b) is the extracted surface

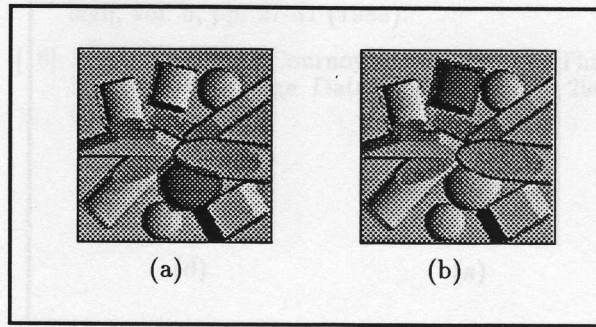


Figure 1: Range images of cat # 105, where the darker regions are the user selected one.

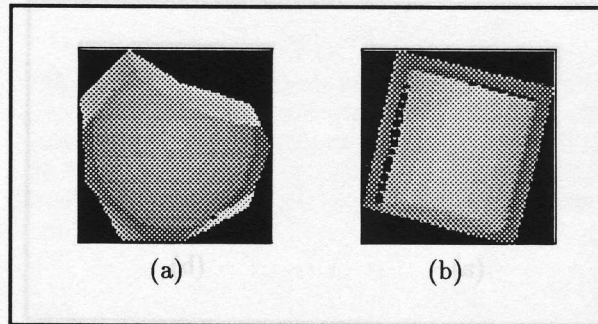


Figure 2: Examples of user selected regions ( $\Omega_0$ ).

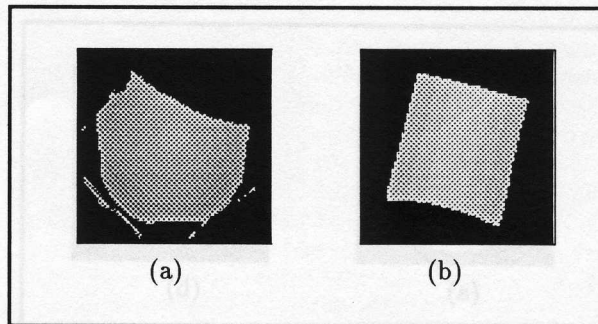


Figure 3: Examples of approximation results of the selected data set by a Bézier surface with  $\|\vec{f}(u_k, v_l) - \vec{z}_{kl}\|^2 \leq T_1$ .

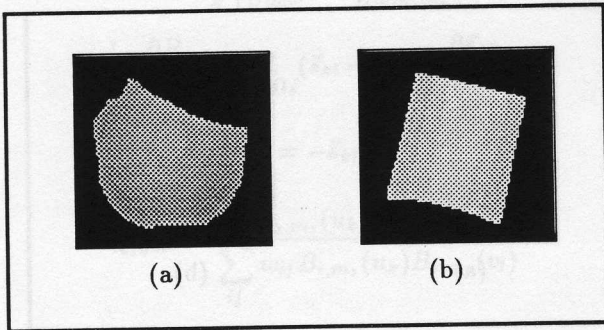


Figure 4: Examples of sub-regions removal from Fig. 3.

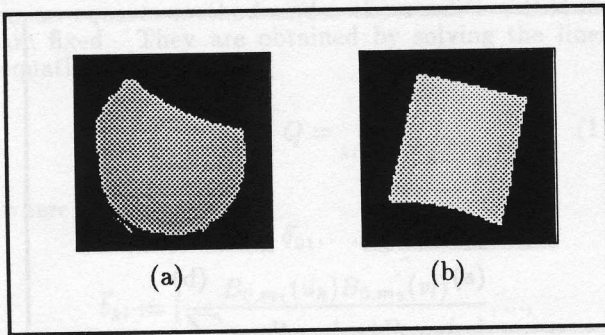


Figure 5: Examples of approximation results using a rational Bézier.

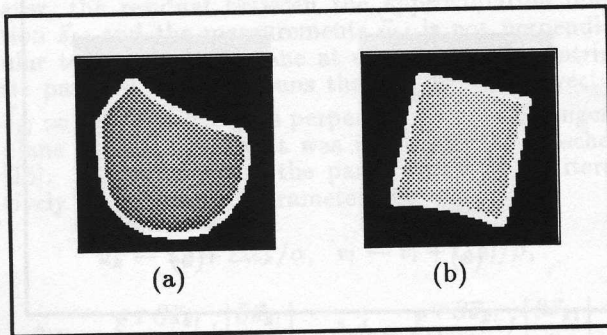


Figure 6: Examples (final results) of sub-regions removal from Fig. 5. The final surfaces are highlighted by a white boundary.

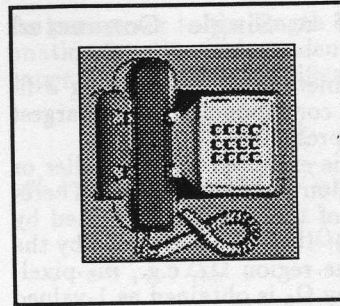


Figure 7: Range image of cat # 028, where the darker region is the user extracted one.

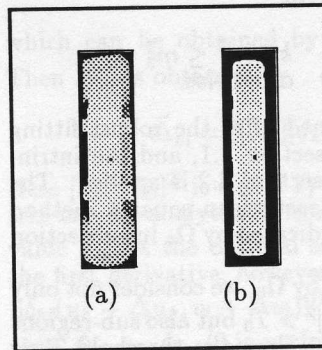


Figure 8: (a) An example of user specified region, (b) an example of the approximated surface using a rational Bézier.

approximated by rational Bézier surface. Here the degrees of the surface and thresholds were the same as in the previous experiments. The upper surface of the handle was well extracted.

## 5. Conclusions

This paper presents a new method for the extraction and approximation of range image data specified interactively. We have demonstrated that we can solve the hard non-linear problem of fitting rational Bézier by the use of an initial Bézier approximation of the data set specified. We have also demonstrated a new intrinsic parametrization algorithm which guaranty that the fitted error is in the direction perpendicular to the local surface tangent. Experimental results show that simple surfaces like cylinders and spheres are well extracted by a rational Bézier surface of degrees  $(2 \times 2)$ .

## 6. Acknowledgement

The authors would like to thank M. Rioux and J. Domey of the National Research Council of Canada (NRCC) who kindly provided access to the range image database. This work is done while one of us (I.S.) is currently enjoying the hospitality of the Autonomous System Laboratory.

## References

- [1] P. Boulanger, G. Godin, and M. Rioux. "Application of 3-D Active Vision to Rapid Prototyping and Reverse Engineering", Third International Conference on Rapid Prototyping, pp.213-223, (1992).
- [2] P. K. Sahoo, S. Soltani and A. K. C. Wong: "A survey of thresholding techniques", *Comput. Vision, Graphics, and Image Proc.*, vol. 41, pp.233-260 (1988).
- [3] R. M. Haralick and L. G. Shapiro: "Image segmentation techniques", *Comput. Vision, Graphics, and Image Proc.*, vol. 29, pp.100-132 (1985).
- [4] S. W. Zucker: "Region growing: childhood and adolescence", *Comput. Graphics and Image Proc.*, vol. 5, pp.382-399 (1976).
- [5] P. J. Besl, R. C. Jain: "Segmentation through variable-order surface fitting", *IEEE Trans. Pattern Anal. Machine Intell.*, vol. 10, no. 2, pp. 167-192 (1988).
- [6] S.S. Sinha and B.G. Schunck. "A Two Stage Algorithm for Discontinuity Preserving Surface Reconstruction". *IEEE Transactions on Pattern Analysis and Machine Intelligence*, Vol. 14, No. 1, (1992).
- [7] P. Boulanger and G. Godin. "Multiresolution Segmentation of Range Images Based on Bayesian Decision Theory", *SPIE Vol. 1825, Intelligent Robots and Computer Vision XI*, pp. 338-350, (1992).
- [8] L. A. Davis: "A survey of edge detection techniques", *Comput. Graphics, and Image Proc.*, vol. 4, pp.248-270 (1975).
- [9] T. Kurita and N. N. Abdelmalek: "An edge-based approach for the segmentation of 3-D range images of small industrial-like objects", *Int. J. Systems Sci.*, vol. 23, no. 9, pp. 1449-1461 (1992).
- [10] G. Roth et M.D. Levine. "Segmentation of geometric signals using robust fitting". 10th International Conference on Pattern Recognition, pp. 826-831, Atlantic City, USA, June (1990).
- [11] P.J. Rousseeuw, et A.M. Leroy. "Robust regression and outlier detection". *J. Wiley & Sons*, (1987).
- [12] E. Lee: "The rational Bézier representation for conics", in G. Farin (Ed.) *Geometric Modeling: Algorithms and New Trends*, SIAM, pp.3-19 (1987).
- [13] R. Sedgewick: "Algorithms in C", Addison Wesley, pp. 115-131 (1990).
- [14] C. R. Giardina and E. R. Dougherty: "Morphological Methods in Image and Signal Processing", Prentice Hall, pp. 36-78 (1988).
- [15] J. Hoschek: "Intrinsic parametrization for approximation", *Computer Aided Geometric Design*, vol. 5, pp. 27-31 (1988).
- [16] M. Rioux and L. Cournoyer: "The NRCC Three-Dimensional Image Data Files", CNRC 29077 (June 1988).